Supplementary Methods, Tables, and Figures

Effect of CYP3A5 Expression on the Inhibition of CYP3A-Catalyzed Drug Metabolism: Impact on CYP3A-Mediated Drug-Drug Interactions

Yoshiyuki Shirasaka, Shu-Ying Chang, Mary F. Grubb, Stephen R. Johnson, Chi-Chi Peng, Kenneth E. Thummel, Nina Isoherranen, and A. David Rodrigues

Inhibition of MDZ 1'-Hydroxylase and TST 6β-Hydroxylase Activity in HLM of *CYP3A5* Genotyped Livers. *Assessment of CYP3A inhibition*. The inhibitory effect of KTZ and ITZ on CYP3A-catalyzed metabolism of MDZ and TST was evaluated using HLMs. The IC_{50} value for KTZ and ITZ in HLM was measured using 1'-hydroxylation of midazolam (1'OH-MDZ) and 6β-hydroxylation of testosterone (6βOH-TST) as probe reactions for CYP3A-catalyzed metabolism. Incubations of each HLM with MDZ or TST were performed in solutions containing 100 mM potassium phosphate buffer (pH 7.4) with 1 mM EDTA in a shaking water bath maintained at 37°C. Conditions that conferred linear metabolite formation, with respect to time under different substrate and HLM protein concentrations, were determined (data not shown) and applied to all kinetic experiments described in this study.

For inhibition experiments with HLM using MDZ as a substrate, MDZ was used at 1 μM, and incubated for 5 min with 0.05 mg/mL HLM protein in a final volume of 100 μL. KTZ and ITZ were added to the 100 μL incubations at final concentrations of 3-3000 nM. All substrates and inhibitors were dissolved in acetonitrile; the final acetonitrile concentration was less than 1%. All reactions were initiated by adding NADPH (final concentration: 1 mM) after 10 min of preincubation and were terminated by adding an equal volume (100 μL) of ice-cold acetonitrile. All incubations were carried out in triplicate. The concentration of 1'OH-MDZ in all samples was quantified with a liquid chromatography-tandem mass spectrometry (LC/MS/MS) system consisting of MDS-Sciex API 3200® triple quadrupole mass spectrometer (AB Sciex, Foster City, CA) coupled with a LC-20AD® ultra fast liquid chromatography (UFLC) system (Shimadzu Co., Kyoto, Japan). The UFLC gradient elution was performed using a mobile phase composed of 0.1% formic acid (A) and acetonitrile (B) at a flow rate of 0.4 mL/min. The gradient profile was 10% B for 0-0.5 min, 10-90% B for 0.5-3.5 min, 90% B for 3.5-5.0 min, 90-10% B for 5.0-5.1 min, and 5.0% B for 5.1-7.0 min. The total run time was 7.0 min for each injection. The retention time of 1'OH-MDZ was 4.0 min. Hypersil GOLD (1.9 μm, 100 × 2.1 mm, Thermo, West Palm Beach, FL) was used as the analytical column. In the LC/MS/MS system, the Turbo Ion Spray interface was operated in the positive ion mode at 5500 V and 450˚C. The mass transition (Q1/Q3) of *m*/*z* 342.107/324.200 was used for 1'OH-MDZ. Analyst software version 1.4 was used for data analysis.

For inhibition experiments with HLM using TST as a substrate, TST was used at 10 μM, and incubated for 10 min with 0.05 mg/mL HLM protein in a final volume of 100 μL. KTZ and ITZ were added to the 100 μL incubations at final concentrations of 1-3000 nM. All substrates and inhibitors were dissolved in acetonitrile; the final acetonitrile concentration was less than 1%. All reactions were initiated by adding NADPH (final concentration: 1 mM) after 10 min of preincubation and were terminated by adding an equal volume (100μL) of ice-cold acetonitrile. All incubations were carried out in triplicate. The concentration of 6βOH-TST in all samples was quantified with a liquid chromatography-tandem mass spectrometry (LC/MS/MS) system consisting of MDS-Sciex API 3200® triple quadrupole mass spectrometer (AB Sciex, Foster City, CA) coupled with a LC-20AD® ultra fast

liquid chromatography (UFLC) system (Shimadzu Co., Kyoto, Japan). The UFLC gradient elution was performed using a mobile phase composed of 0.1% formic acid (A) and acetonitrile (B) at a flow rate of 0.3 mL/min. The gradient profile was 5.0% B for 0-2.0 min, 5.0-100% B for 2.0-4.0 min, 100% B for 4.0-5.5 min, 100-5.0% B for 5.5-5.6 min, and 5.0% B for 5.6-9.0 min. The total run time was 9.0 min for each injection. The retention time of 6βOH-TST was 4.5 min. ZORBAX (SB-C_{18} 5 µm, 2.1 x 50 mm, Agilent Technologies, Palo Alto, CA) was used as the analytical column. In the LC/MS/MS system, the Turbo Ion Spray interface was operated in the positive ion mode at 5500 V and 450˚C. The mass transition (Q1/Q3) of *m*/*z* 305.186/287.200 was used for 6βOH-TST. Analyst software version 1.4 was used for data analysis.

Determination of IC_{50}. The inhibitory effects of KTZ and ITZ on CYP3A-catalyzed metabolism of MDZ and TST were expressed as percent of control activity. Percent of control activity was determined as the ratio of the amount of 1'OH-MDZ and 6βOH-TST in the presence to that in the absence of KTZ or ITZ. The KTZ and ITZ concentrations giving half-maximum inhibition (IC_{50}) were obtained by means of nonlinear least-squares analysis using Graphpad prism (Peng et al 2012) or the MULTI program (Yamaoka et al., 1981).

Peng CC, Shi W, Lutz JD, Kunze KL, Liu JO, Nelson WL, and Isoherranen N (2012) Stereospecific metabolism of itraconazole by CYP3A4: dioxolane ring scission of azole antifungals. *Drug Metab Dispos* **40**:426-435.

Yamaoka K, Tanigawara Y, Nakagawa T, and Uno T (1981) A pharmacokinetic analysis program (multi) for microcomputer. *J Pharmacobiodyn* **4**: 879-885.

Reconstitution of Purified Wild-Type and Mutant CYP3A4 with P450 Reductase and Cytochrome b_5. Purified CYP3A4 (wild-type, mutant F213W, and L211F/D214E) was reconstituted with purified NADPH-P450 reductase, and cytochrome b_5 (molar ratio of 1:4:2), as described previously (Domanski et al, 2001), in the presence of 3-[(3-cholamidopropyl)dimethylammonio]-1-propanesulfonate (4%) and dioleoyl phosphatidylcholine (0.1 mg/mL) in 100 mM 3-(N-morpholino)propanesulfonic acid buffer (pH 7.6). TST 6β-hydroxylase activity (TST concentration of 25 and 100 µM) was determined after dilution of the reconstitution mixture in 50 mM 4-(2-hydroxyethyl)-1-piperazineethanesulfonic acid (pH 7.6) containing $MgCl_2$ (15 mM) and 0.1 mg/mL dioleoyl phosphatidylcholine. The final concentration of CYP3A4, P450 reductase and cytochrome b_5 was 0.5, 2, and 1 nM, respectively. The IC_{50} values for ITZ were obtained at two concentrations of TST (25 and 100 µM).

Domanski TL, He YA, Khan KK, Roussel F, Wang Q, and Halpert JR (2001) Phenylalanine and tryptophan scanning mutagenesis of CYP3A4 substrate recognition site residues and effect on substrate oxidation and cooperativity. *Biochemistry* **40**:10150-10160.

Determination of Ligand-Induced Binding Spectra. The binding mode and affinity of the ITZ and KTZ was determined by spectral titration with rCYP3A4 and rCYP3A5 Supersomes (Kunze et al., 2006). The ligand-induced binding spectra (difference spectra) were recorded with a Varian Cary 3E UV-Vis spectrophotometer. Matched cuvettes containing CYP3A4 or CYP3A5 Supersomes (200nM P450) in 100mM potassium phosphate buffer (pH 7.4) at 22°C were used. ITZ and KTZ (10 nM-6.5 µM) were added in 1 µL increments to the sample cuvette and the same volume of solvent (acetonitrile) was added to the reference cuvette. Ligand-induced difference spectra were recorded and, due to the tight binding of both azoles, the Ks values were obtained by fitting the "Morrison" equation (Eq. S1) to the spectral titration data. The enzyme-ligand (EL) complex concentration was determined by Lambert-

Beer law using the extinction coefficient determined from maximum absorbance detected when the P450 protein was saturated, as previously described (Kunze et al., 2006) (Eq. S1).

$$[\mathrm{EL}] = \frac{[\mathrm{E}] + [\mathrm{L}] + K_s - \sqrt{([\mathrm{E}] + [\mathrm{L}] + K_s)^2 - 4[\mathrm{E}]\ \mathrm{x}\ [\mathrm{L}]}}{2} \qquad \text{(S1)}$$

Ks is the affinity constant of the ligand, [L] is the concentration of ligand, [E] is the concentration of enzyme, and [EL] is the concentration of the enzyme-ligand complex.

Kunze KL, Nelson WL, Kharasch ED, Thummel KE, and Isoherranen N (2006) Stereochemical aspects of itraconazole metabolism in vitro and in vivo. *Drug Metab Dispos* **34**:583-590.

Table S1

Summary of Curve Fitting and IC_{50} Determination for KTZ with rCYP3A4 and rCYP3A5

Substrate	P450	[S]	Mean IC_{50}	±SD	R^2	Min	Max	Slope (y)
MDZ	CYP3A4	1.4	0.04	0.01	0.996	2.7	100	-1.5
		0.1	0.002	0.0002	0.999	0	100	-1.0
	CYP3A5	2.7	0.2	0.004	0.999	0	100	-0.9
		0.2	0.017	0.003	0.993	0	100	-0.9
TST	CYP3A4	78	0.009	0.001	0.990	0	100	-0.7
		4	0.016	0.0007	0.997	0	100	-1.3
	CYP3A5	67	0.04	0.006	0.991	0	100	-0.7
		3	0.08	0.007	0.986	0	100	-0.8
Terfenadine	CYP3A4	2.4	0.09	0.005	0.999	0	100	-1.0
		0.2	0.0082	0.001	0.996	0	100	-0.9
	CYP3A5	1.2	0.2	0.005	0.999	0	100	-0.9
		0.1	0.0065	0.002	0.968	0	100	-0.7
Vincristine	CYP3A4	85	0.15	0.03	0.970	0	100	-1.3
		4	0.11	0.01	0.991	0	100	-2.3
	CYP3A5	45	0.12	0.01	0.997	0	100	-0.6
		2	0.07	0.01	0.983	0	100	-2.1

IC_{50} values (± SD) were obtained at two [S] by means of nonlinear least-squares analysis (Eq. S2) using XLfit (IDBS, Guildford, UK).

$$y = \min + \frac{\max - \min}{1 + \left(\frac{x}{IC_{50}}\right)^{-y}} \quad \text{(S2)}$$

Where IC_{50} is the "*x*" value for the point in the curve that is midway between the "*max*" (maximum activity remaining; minimal % inhibition) and "*min*" (minimal activity remaining; maximal % inhibition). The exponent "*y*" is the slope of the curve at its midpoint. IC_{50} plots are shown (Figures S2 and S4).

Table S2

Summary of Curve Fitting and IC_{50} Determination for ITZ with rCYP3A4 and rCYP3A5

Substrate	P450	[S]	Mean IC_{50}	±SD	R^2	Min	Max	Slope (y)
MDZ	CYP3A4	1.4	0.24	0.05	0.999	5.3	100	-1.4
		0.1	0.005	0.001	0.984	0	100	-0.7
	CYP3A5	2.7	2.3	0.4	0.987	0	100	-0.7
		0.2	0.15	0.04	0.994	0	100	-0.9
TST	CYP3A4	78	0.04	0.007	0.985	0	100	-1.1
		4	0.045	0.003	0.995	0	100	-1.3
	CYP3A5	67	1.3	0.4	0.967	0	100	-0.8
		3	0.41	0.18	0.940	0	100	-0.4
Terfenadine	CYP3A4	2.4	0.9	0.2	0.999	16	100	-1.7
		0.2	0.023	0.004	0.995	0	100	-1.0
	CYP3A5	1.2	2.1	0.5	0.999	33	100	-2.0
		0.1	0.064	0.014	0.972	0	100	-0.8
Vincristine	CYP3A4	85	0.36	0.05	0.986	0	100	-0.9
		4	0.029	0.004	0.993	0	100	-1.7
	CYP3A5	45	0.68	0.23	0.926	0	100	-0.6
		2	0.05	0.005	0.992	0	100	-1.0

IC_{50} values (± SD) were obtained at two [S] by means of nonlinear least-squares analysis (Eq. S2) using XLfit (IDBS, Guildford, UK).

$$y = \min + \frac{\max - \min}{1 + \left(\frac{x}{IC_{50}}\right)^{-y}} \quad \text{(S2)}$$

Where IC_{50} is the "*x*" value for the point in the curve that is midway between the "*max*" (maximum activity remaining; minimal % inhibition) and "*min*" (minimal activity remaining; maximal % inhibition). The exponent "*y*" is the slope of the curve at its midpoint. IC_{50} plots are shown (Figures S1 and S3).

Table S3

ITZ as an Inhibitor of Fully Reconstituted Wild-Type and Mutant CYP3A4

CYP3A4 Preparation	Kinetic Profile[b]	IC_{50} (nM)[a] TST (25 μM)	IC_{50} (nM)[a] TST (100 μM)
Wild-Type	Sigmoidal	81 ± 16	140 ± 62
F213W	NR	92 ± 30[c]	79 ± 14[d]
L211F/D214E	Hyperbolic	65 ± 7.0[c]	80 ± 13[*]

[a]IC_{50} was determined at two concentrations of TST and is presented as the mean ± S.D. (n = 3 determinations).
[b]TST profile reported previously for wild-type and L211F/D214E forms of CYP3A4 (Harlow and Halpert, 1998).
NR: Not reported.
[c]Not statistically significant versus wild-type (P = 0.16, L211F/D214E; P = 0.26, F213W).
[d]Not statistically significant versus wild-type (P = 0.05).
* P <0.05 (P = 0.04), significantly different from wild-type CYP3A4.

Harlow GR and Halpert JR (1998) Analysis of human cytochrome P450 3A4 cooperativity: construction and characterization of a site-directed mutant that displays hyperbolic steroid hydroxylation kinetics. *Proc Natl Acad Sci U S A* **95**: 6636-6641.

Supplement Figure S1

Representative IC_{50} plots describing the inhibition of rCYP3A4- and rCYP3A5-catalyzed metabolism of MDZ, TST, terfenadine and vincristine by ITZ ([S]/K_m ratio ~1.0)

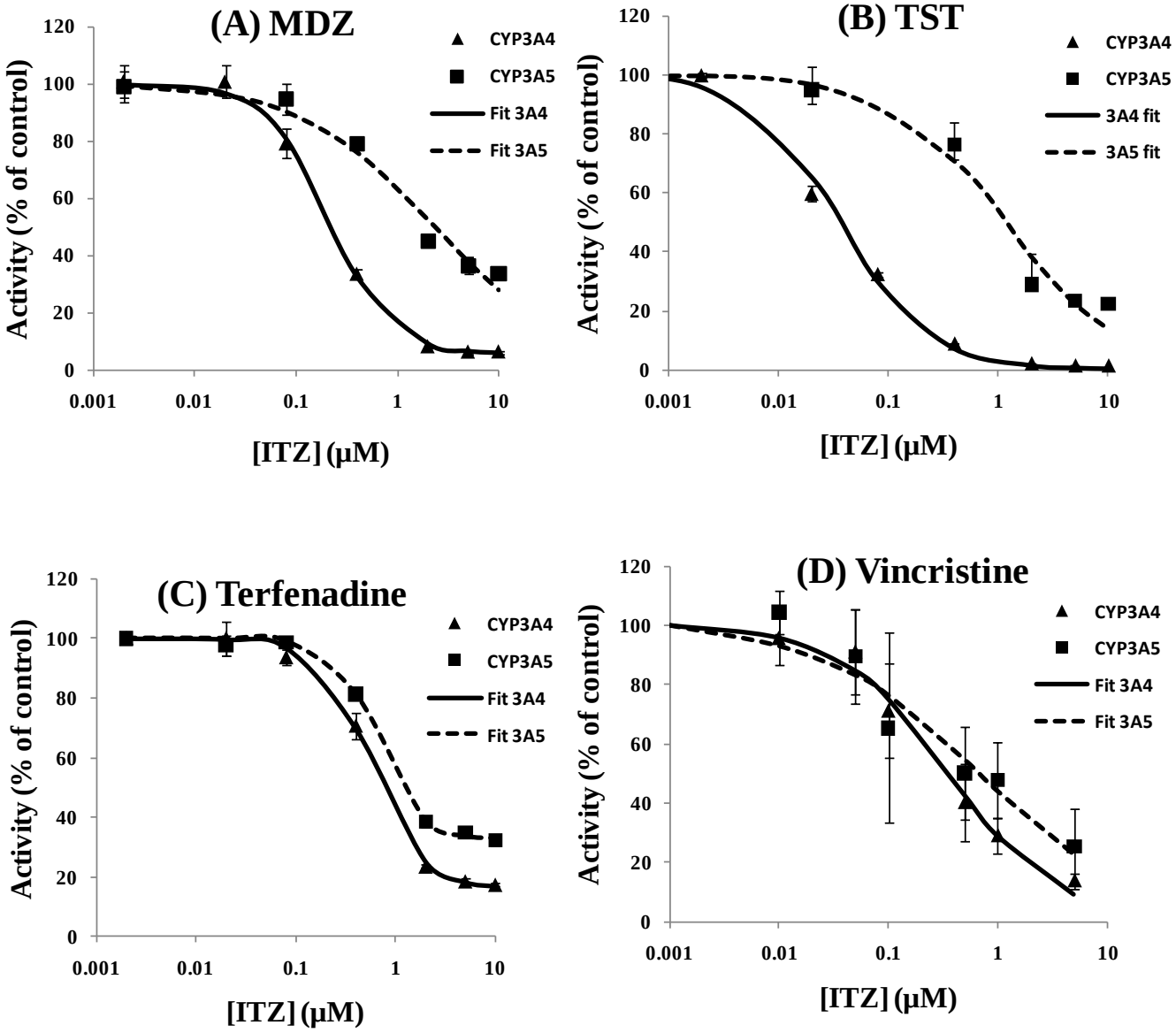

Supplement Figure S2

Representative IC_{50} plots describing the inhibition of rCYP3A4- and rCYP3A5-catalyzed metabolism of MDZ, TST, terfenadine and vincristine by KTZ ([S]/K_m ratio ~1.0)

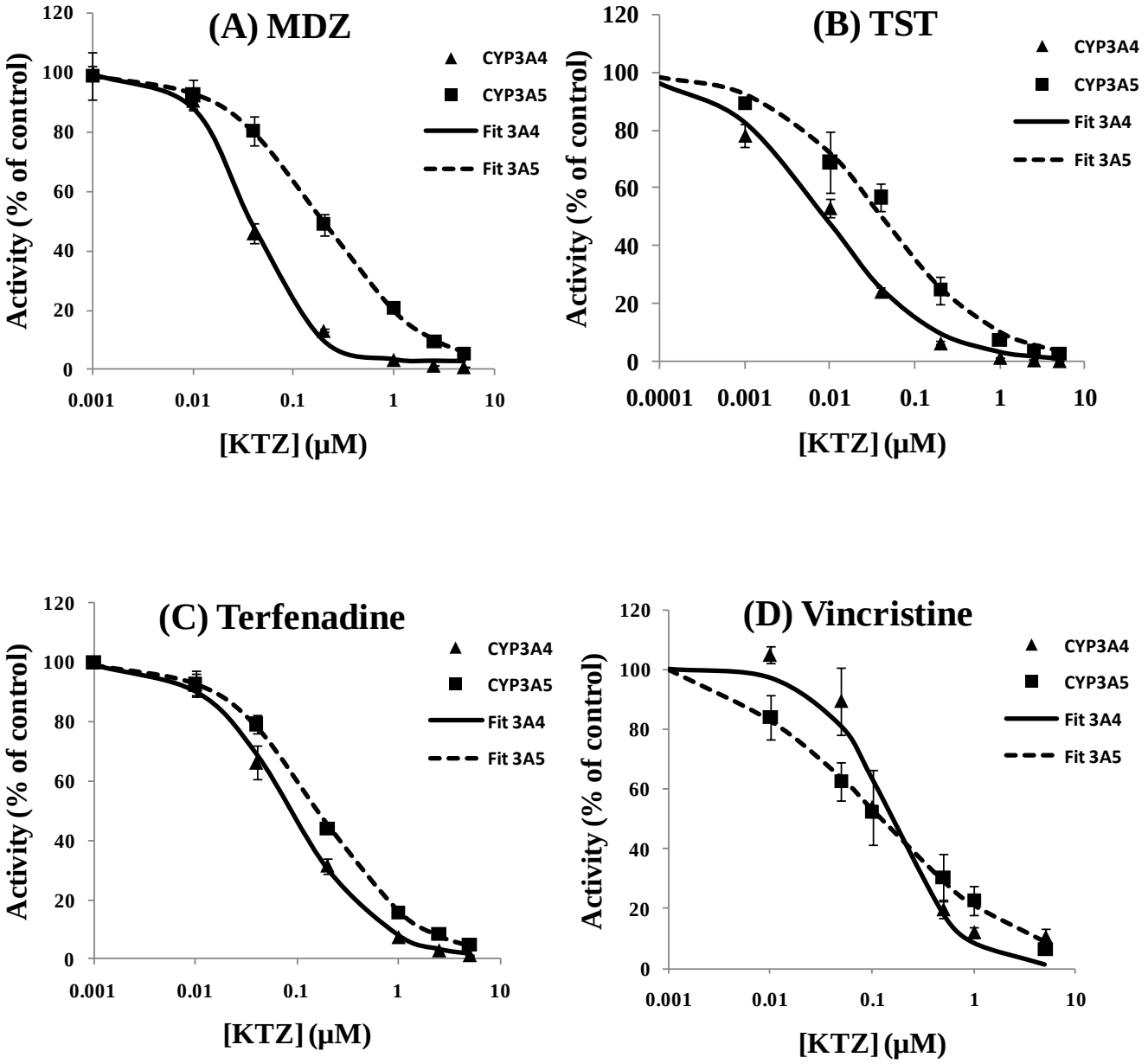

Supplement Figure S3

Representative IC_{50} plots describing the inhibition of rCYP3A4- and rCYP3A5-catalyzed metabolism of MDZ, TST, terfenadine and vincristine by ITZ ([S]/K_m ratio ~0.05)

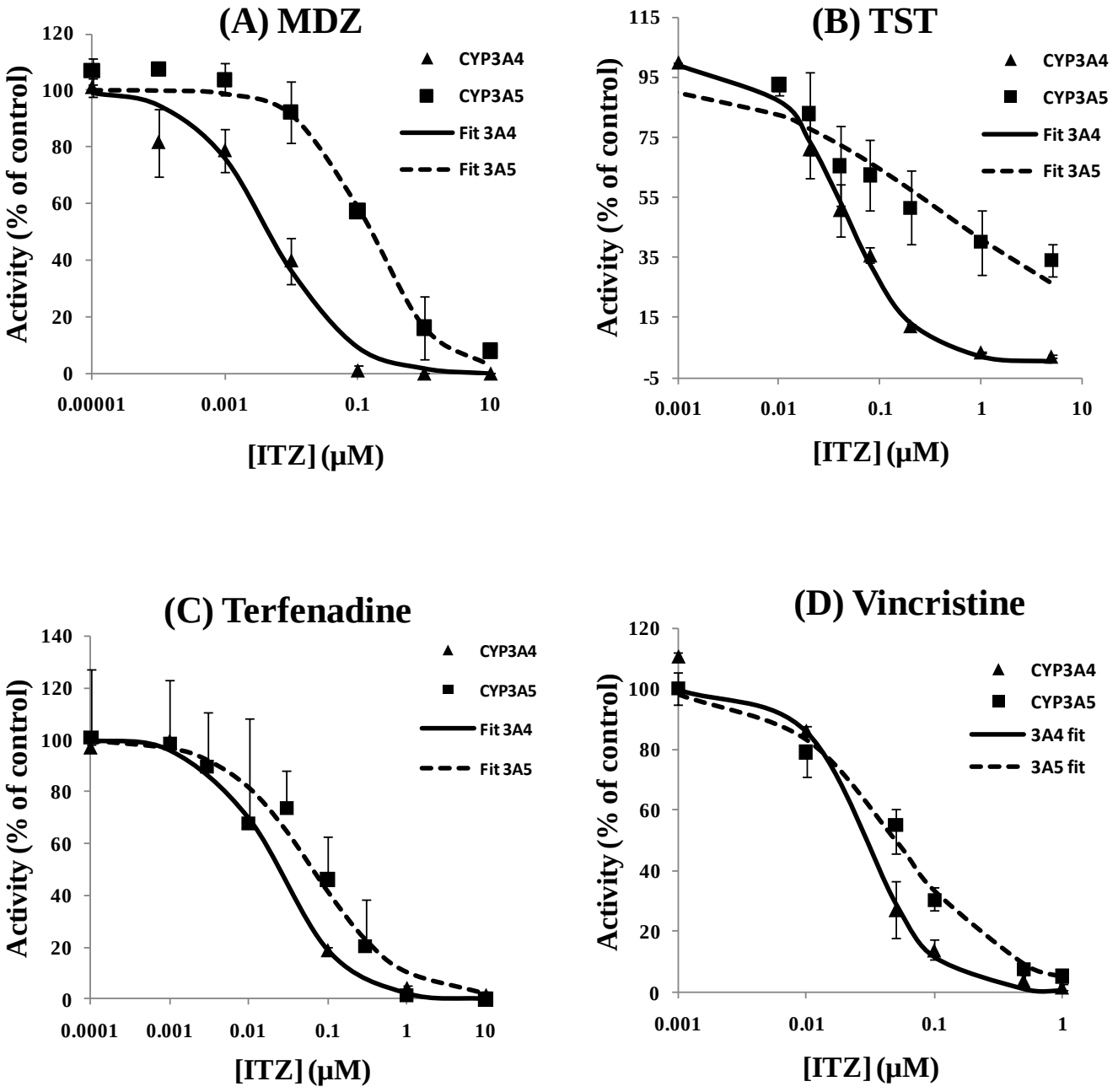

Supplement Figure S4

Representative IC_{50} plots describing the inhibition of rCYP3A4- and rCYP3A5-catalyzed metabolism of MDZ, TST, terfenadine and vincristine by KTZ ([S]/K_m ratio ~0.05)

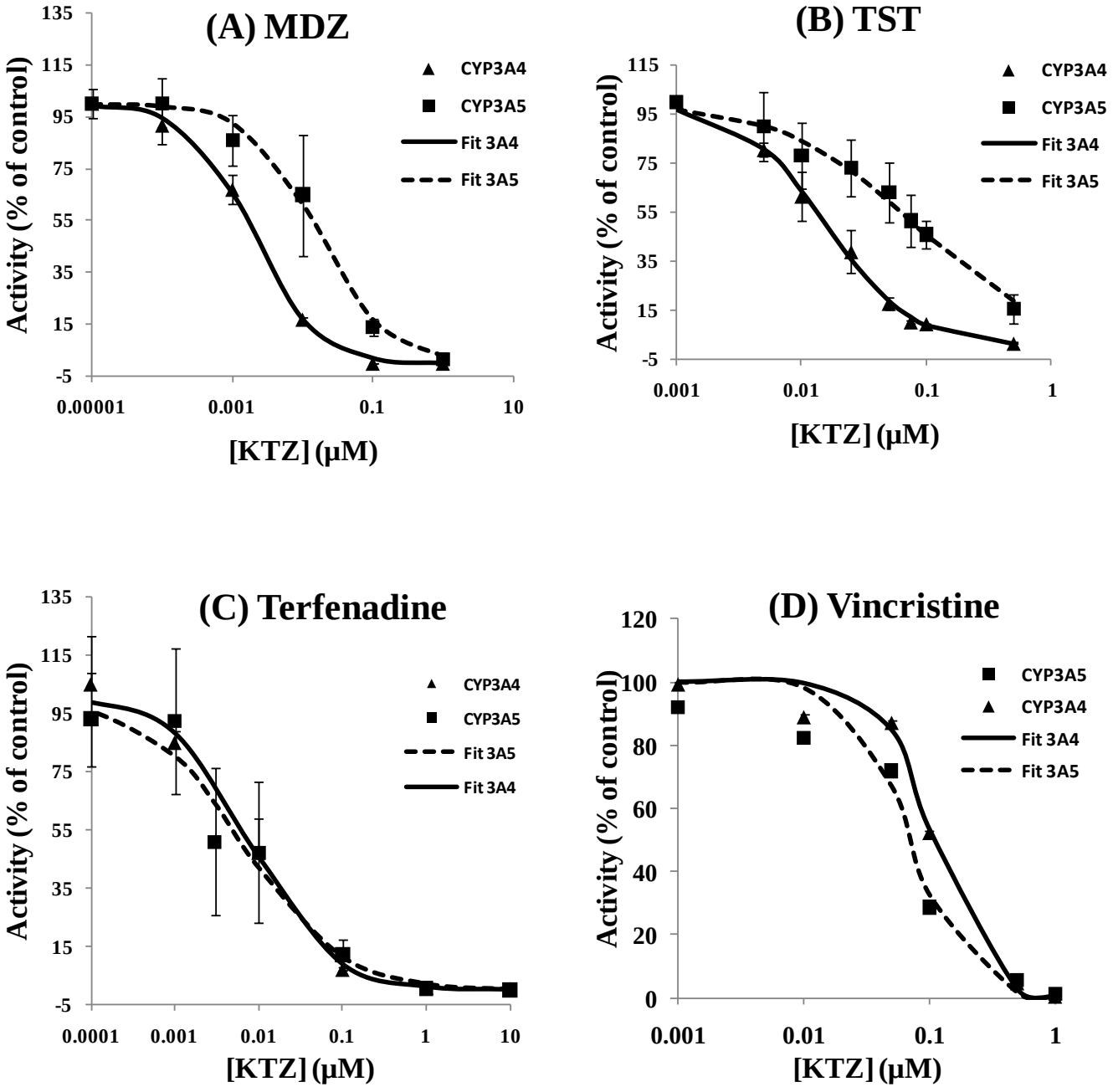

Supplement Figure S5

Representative Type II ligand spectral titration plot for ITZ with rCYP3A4 (A) and rCYP3A5 (B) and KTZ with rCYP3A4 (C) and rCYP3A5 (D)

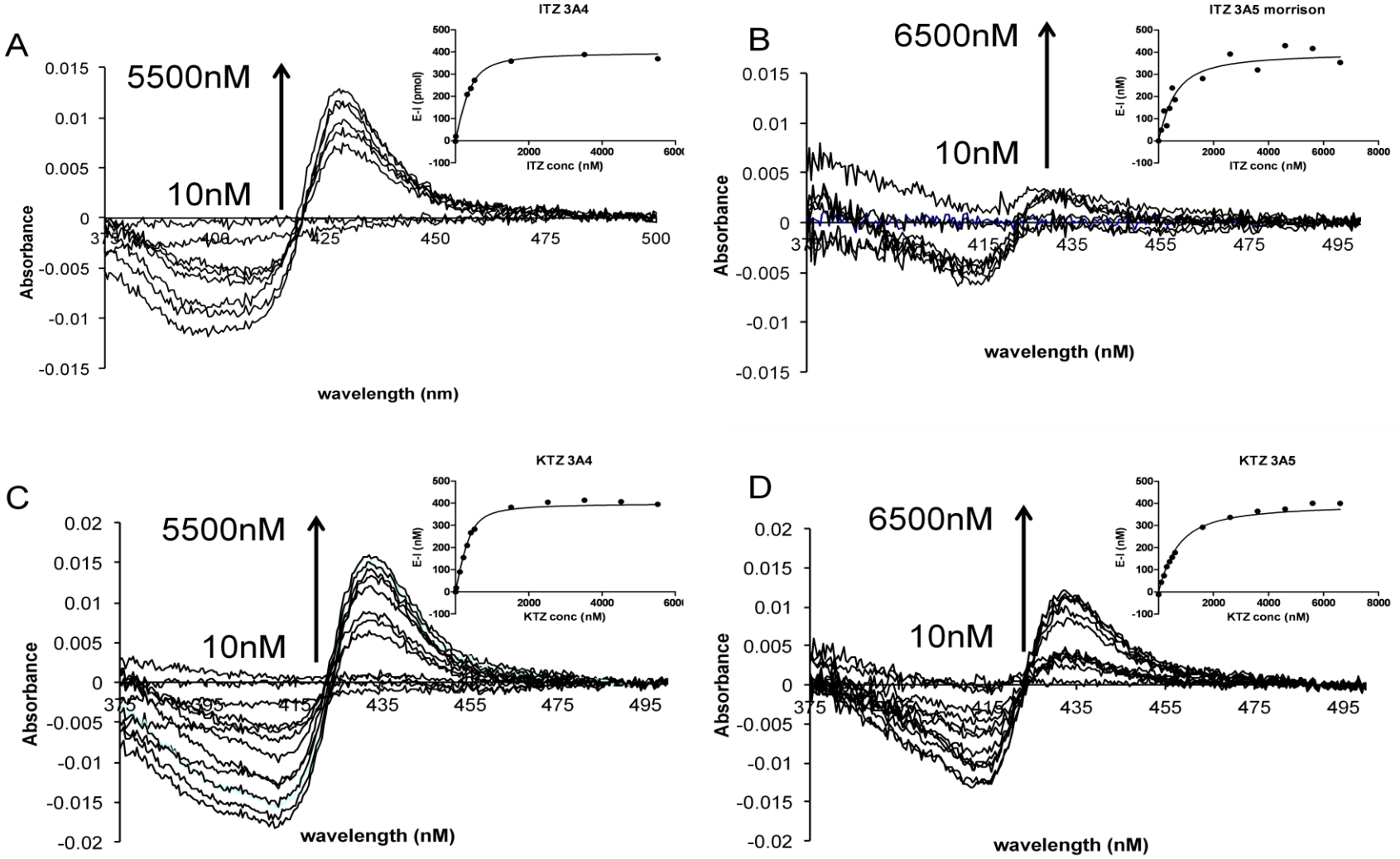

Supplement Figure S6

Representative IC_{50} plots describing the inhibition wild-type and mutant CYP3A4-catalyzed TST (25 and 100 µM) metabolism by ITZ

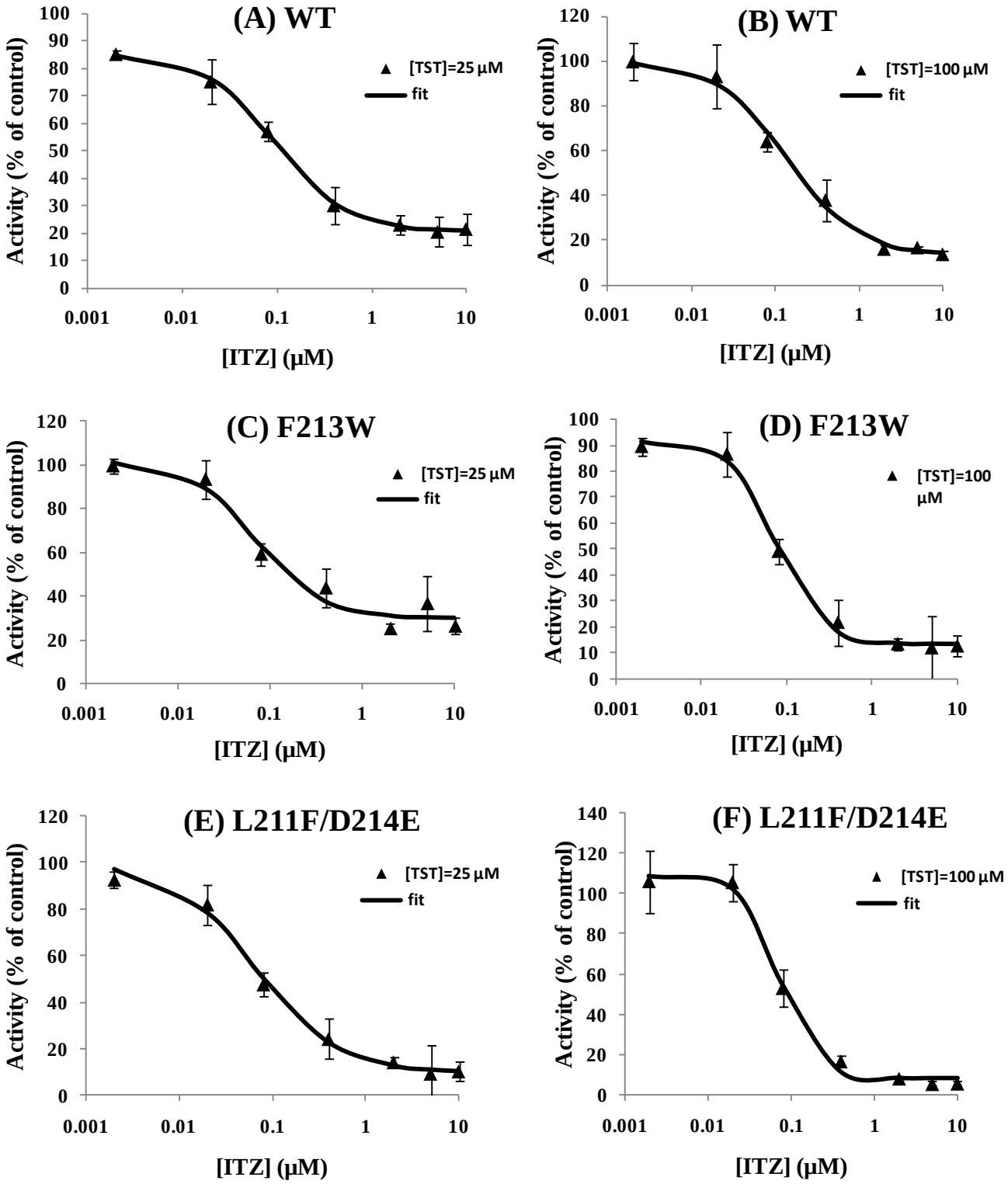

Supplement Figure S7

Representative IC_{50} plots describing the inhibitory effect of KTZ and ITZ on CYP3A-catalyzed metabolism of MDZ in HLM

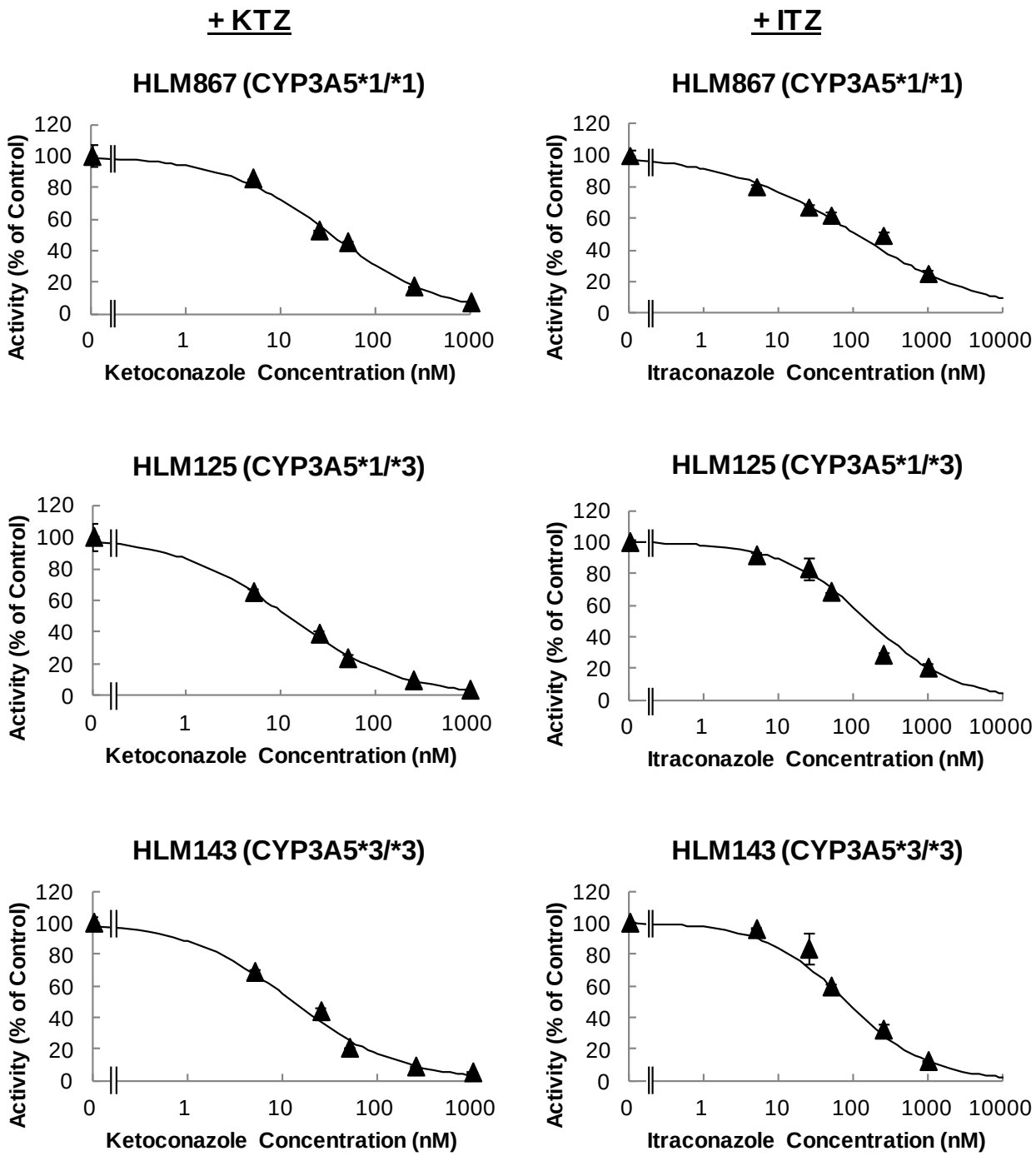

Supplement Figure S8

Representative IC_{50} plots describing the inhibitory effect of KTZ and ITZ on CYP3A-catalyzed metabolism of TST in HLM